Including Smart Loads for Optimal Demand Response in Integrated Energy Management Systems for Isolated Microgrids

Bharatkumar V. Solanki, *Student Member, IEEE,* Akash Raghurajan, Kankar Bhattacharya, *Senior Member, IEEE,* and Claudio A. Cañizares, *Fellow, IEEE*

***Abstract*—This paper presents a mathematical model of smart loads in demand response (DR) schemes, which is integrated into centralized Unit Commitment (UC) with Optimal Power Flow (OPF) coupled Energy Management Systems for isolated microgrids for optimal generation and peak load dispatch. The smart loads are modeled with a neural network (NN) load estimator as a function of the ambient temperature, time of day, Time of Use (TOU) price, and the peak demand imposed by the microgrid operator. To develop the NN-based smart load estimator, realistic data from an actual Energy Hub Management System (EHMS) is used for supervised training. Based on these, a novel Microgrid Energy Management System (MEMS) framework based on a Model Predictive Control (MPC) approach is proposed, which yields optimal dispatch decisions of dispatchable generators, energy storage system (ESS), and peak demand for controllable loads, considering power flow and UC constraints simultaneously. To study the impact of DR on the microgrid operation with the proposed MEMS framework, a CIGRE benchmark system is used that includes distributed energy resources (DERs) and renewables based generation. The results show the feasibility and benefits of the proposed models and approach.**

***Index Terms*—Demand response, home energy management systems, smart loads, energy management systems, microgrids.**

NOMENCLATURE

Indices and Superscripts

g	Generating units
i, j	Bus
k_t	Time-step [min]
n	ESS units
t	Time [min]
x	Input layer neurons of NN, $x \in X$
y	Hidden layer neurons of NN, $y \in Y$
^{c}	Commercial
^{r}	Residential

Sets

G_i	Generator units connected to bus *i*
N_i	ESS units connected to bus *i*

Parameters

a_g	Quadratic term of cost function [\$/kWh^2]
B^{op}	NN bias at the output neuron
B^{ip}_y	NN bias at the hidden layer neuron
b_g	Linear term of cost function [\$/kWh]
C^{LC}	Load curtailment cost [\$/kWh]
C^{sdn}_g	Shut-down cost generating units [\$]
C^{sup}_g	Start-up cost generating units [\$]
c_g	Constant term of cost function [\$/h]
$IP_{x,t}$	NN input
$IW_{x,y}$	Hidden layer weights of NN
$K_{1,2}$	Reactive power load factors [kVAR/kW]
LW_y	Output layer weights of NN
PD_{i,k_t}	Active power demand [p.u.]
PW_{i,k_t}	Wind turbine output [p.u.]
$\overline{PESS}_n$	Maximum charging/discharging power limit of ESS [p.u.]
PV_{i,k_t}	Photovoltaic unit output [p.u.]
R^{dn}_g	Ramp down rate of generating units [p.u./h]
R^{up}_g	Ramp up rate of generating units [p.u./h]
T^{dn}_g	Minimum down time of generating units [h]
T^{up}_g	Minimum up time of generating units [h]
α_{k_t}	Voltage exponent for active load
β_{k_t}	Voltage exponent for reactive load
Δt_{k_t}	Absolute time between step k_t and step k_{t+1} [h]
η^{ch}_n	Charging efficiency of ESS
η^{dch}_n	Discharging efficiency of ESS
γ_{k_t}	Errors in the output of the RCLPE [p.u.]
$\underline{\cdot}, \overline{\cdot}$	Minimum, maximum variable limits

Variables

P_{g,k_t}	Active power from generating units [p.u.]
P^{ch}_{n,k_t}	ESS charging power [p.u.]
P^{dch}_{n,k_t}	ESS discharging power [p.u.]
$P^{LC}_{k_t}$	Load curtailed [p.u.]
$P^{max}_{k_t}$	Demand limit - DR control [kW]
$PD^{rc}_{k_t}$	Residential controllable active power demand [p.u.]
Q_{g,k_t}	Reactive power from generating units [p.u.]
QC_{n,k_t}	ESS reactive power output [p.u.]
$\mathcal{S}_{i,j,k_t}$	Apparent power transfer between i and j [p.u.]
S_{g,k_t}	Shut-down decision (1 = shut-down, 0 = otherwise)
SOC_{n,k_t}	State of charge of ESS [p.u.]
$U_{g.k_t}$	Start-up decision (1 = start-up, 0 = otherwise)
V_{i,k_t}	Bus voltage [p.u.]

This work has been supported by NSERC Smart Microgrid Network (NSMG-NET), Canada.

The authors are with the Department of Electrical and Computer Engineering, University of Waterloo, ON, N2L3G1, Canada (e-mail: {b2solanki, araghura, kankar, ccanizar}@uwaterloo.ca).

W_{g,k_t} ON/OFF decision (1 = ON, 0 = OFF)
δ_{i,k_t} Voltage angle [radian]

I. Introduction

THERE are many remote communities around the world which do not have interconnection with the power grid because of technical and/or economic constraints, and thus have to manage their energy requirements independently, mainly from fossil-fuel based and, in some cases, renewable based generations. Such systems operate as isolated microgrids.

A microgrid is a group of interconnected loads and Distributed Energy Resources (DERs) such as distributed generators (DGs), energy storage systems (ESS) and controllable loads, within a clearly defined and local electrical boundary that can act as a single controllable entity with respect to the grid [1]. The reliable and economic operation of a microgrid is handled by an Energy Management System (EMS), which includes scheduling and dispatching of DGs while maintaining appropriate reserve levels, and considering uncertainty in the forecast of renewable and coordination of DERs and demand response (DR) management [2], [3].

The concept of centralized EMS for microgrids, based on Unit Commitment (UC) and Optimal Power Flow (OPF) models, have been reported. UC based EMS models in [4] and [5] take into account the operational constraints pertaining to DERs such as ramp-up, ramp-down, and minimum up/down-time constraints, but do not consider network flows; on the other hand, the OPF based EMS models in [6] and [7] do consider the network flows, but do not consider the above mentioned operational constraints. A UC based centralized microgrid EMS with the objective of simultaneously reducing fuel consumption and pollutant emissions is presented in [4], considering photovoltaic (PV) based and fossil fuel based DGs and ESS. In [5], a UC based EMS is proposed to determine optimal dispatch of DGs and ESS, and purchase/sell decisions with the objective of minimizing the microgrid operation costs. In [6], an OPF based EMS for grid connected industrial microgrids is proposed, which considers revenue maximization and includes constraints associated with power flows, ESS, and plug-in electric vehicles. Paper [7] describes a multi-objective OPF problem for optimal dispatch of DGs and ESS in the presence of renewable based generation for isolated microgrids. None of the above mentioned references consider DR as an option in the proposed EMS frameworks.

Customer participation in energy management, enabled by DR mechanisms [8], can play a key role in improving the efficiency of operation of isolated microgrids and facilitate the integration of renewables. Thus, in [9], the impacts of residential DR on network losses, voltage profiles, and service reliability in distribution networks are studied by considering aggregated load profiles in a power flow analysis problem, which are developed using realistic metered usage data and load profile flexibility estimated from surveyed data. The impact of price-responsive and controllable loads in a three-phase unbalanced distribution system is discussed in [10], formulating a Distribution Optimal Power Flow (DOPF) model. In [11], the demand behaviour in response to real time pricing (RTP) is expressed by price elasticity coefficients; the energy management problem considers linearized power flow and UC constraints simultaneously. However, works [9]–[11] do not take into account ESS and renewable based DGs. On the other hand, the effect of different DR options on the operation of isolated microgrids, such as peak shaving and demand shifting, are modeled in [12] by using associated cost and price elasticity coefficients. Although the work considers DR and renewables DGs in the EMS framework, it does not include ESS.

For isolated microgrids with a high penetration of renewables based DGs, deviations in the forecast of renewables can significantly affect the dispatch decisions of other resources and hence operating costs [3]. Therefore, the microgrid EMS needs to re-evaluate the dispatch decisions at frequent intervals considering the deviations from forecasts. Recently, Model Predictive Control (MPC) has found significant applications in systems with uncertain inputs, wherein the optimization problem is solved at discrete time steps considering updated forecasted inputs with a rolling time horizon, with the obtained optimal decisions being only valid for the next time step [13]. In [14], the energy management problem of an isolated microgrid is decomposed into UC and OPF sub-problems; in order to address the uncertainty in the forecast of wind and solar PV generation, an MPC technique is adopted in which the EMS is solved every 5 min considering updated forecasted inputs and moving forward the time horizon. However, the proposed EMS does not consider load curtailment or control mechanisms. In [15] and [16], UC based EMS models for renewables based microgrids are presented, in which the variation in the forecast of renewables and demand is accounted for by applying an MPC approach. A component of the electricity demand is considered shiftable to other hours [15], which is a form of DR. On the other hand, in [16], two types of loads are represented: critical loads, which are fixed, and controllable loads, which can be curtailed, based on a cost to account for user discomfort.

In [9]–[12], [15] and [16], DR is included in the EMS by modeling controllable loads either by price elasticity coefficients or by curtailment with an associated cost. However, such representations fail to capture the load behaviour in response to various DR controls such as peak demand limits, or externalities such as weather conditions. Therefore, in this paper, a neural network (NN) based Residential Controllable Load Profile Estimator (RCLPE) is presented, which is developed using measured and simulated data from an actual Energy Hub Management System (EHMS) [17], and represents controllable loads that respond to various DR controls, in particular peak demand constraints. Moreover, to investigate the economic and technical impact and benefits of some DR schemes, the developed NN-based RCLPE is integrated within a UC-OPF coupled Microgrid Energy Management System (MEMS) framework, which yields the optimal dispatch of DGs, ESS, and controllable loads considering power flow and UC operational constraints simultaneously. To account for the uncertainties in the forecast of renewables and demand, an MPC approach is adopted. The effectiveness of the proposed

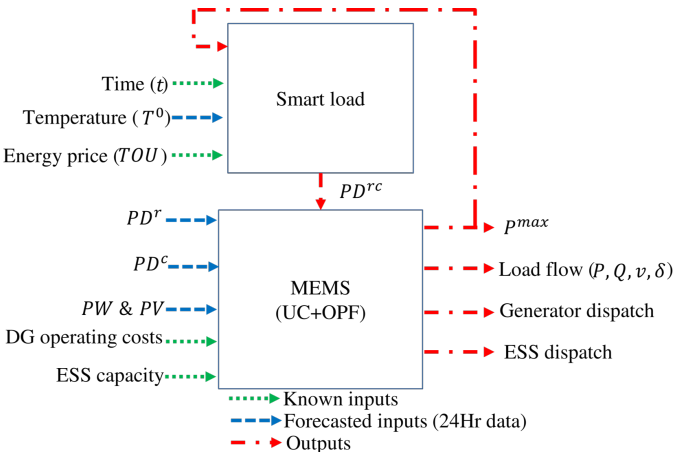

Fig. 1. Proposed MEMS architecture.

framework is compared with traditional EMS approaches, which separate the EMS problem in UC and OPF sub-problems. Hence, the main contributions of this work are as follows:

- An RCLPE is developed by using supervised NN learning to estimate the demand of smart loads as a function of ambient temperature, TOU price, time of the day, and peak demand constraints imposed by the microgrid operator (MGO).
- The estimated NN load model from the RCLPE is incorporated into an integrated MEMS framework to study the impact and potential of smart DR.
- A comprehensive mathematical formulation of the optimal EMS for isolated microgrids, which simultaneously considers power flow and UC operational constraints, is proposed and demonstrated.
- An MPC approach is applied to the proposed MEMS framework to take into account the uncertainties associated with renewables and electricity demand.

The rest of the paper is organized as follows: Section II presents the architecture of the proposed MEMS, and the mathematical model of the coupled UC+OPF microgrid dispatch approach. Section III discusses the decoupled version of the proposed MEMS, its time horizon, and its MPC implementation. Section IV describes the proposed RCLPE, while Section V presents the test system considered, and discusses some of more relevant results obtained with the proposed MEMS, highlighting its main features and demonstrating its feasibility. Finally, Section VI highlights the main conclusions and contributions of this paper.

II. Proposed MEMS

The proposed MEMS architecture for an isolated microgrid is shown in Fig. 1, comprising the smart loads and the MEMS itself. The introduced controllable load demand PD^{rc} is a function of the ambient temperature (T^0), TOU price, peak demand constraint (P^{max}), and the time of day; among them, the time of the day and the TOU prices are known inputs, T^0 is a forecasted input, and P^{max} is a variable determined optimally by the MEMS.

One of the main outputs of the MEMS model is the dispatch of the controllable demand as an available resource. The other MEMS outputs are the dispatch of available resources in the microgrid considering the operational limits and constraints related to the dispatchable units, power flows, ESS energy balance, and spinning reserve requirements.

The mathematical model of MEMS is comprised of an objective function that represents the microgrid operational cost, including generation costs, start up and shut down costs, and costs associated with load curtailment, as follows:

$$J = \sum_{g,k_t}[(a_g P_{g,k_t}^2 \Delta t_{k_t} + b_g P_{g,k_t} + c_g W_{g,k_t})\Delta t_{k_t} + C_g^{sup} U_{g.k_t} + C_g^{sdn} S_{g,k_t}] + \sum_{i,k_t} P_{k_t}^{LC} C^{LC} \Delta t_{k_t} \quad (1)$$

where all variables and parameters in their and other equations are defined in the Nomenclature section. It is assumed that the MGO owns all the DERs, and fully controls them. Furthermore, load curtailment is considered in (1) with significant high cost. The above objective function is subjected to the constraints discussed next.

A. Real and Reactive Power Balance

The real power balance at a bus considers the output from DG, solar PV and wind units, and the net power of the loads from commercial and residential customers, taking into account ESS charging and discharging, and the network flows, as follows:

$$\sum_{g\in G_i} P_{g,k_t} W_{g,k_t} + PV_{i,k_t} + PW_{i,k_t} - PD_{i,k_t}^c V_{i,k_t}^{\alpha_{k_t}^c} - [PD_{i,k_t}^r + PD_{i,k_t}^{rc}(P_{k_t}^{max}) - P_{k_t}^{LC}] V_{i,k_t}^{\alpha_{k_t}^r} + \sum_{n\in N_i}(P_{n,k_t}^{dch} - P_{n,k_t}^{ch}) = \sum_j V_{i,k_t} V_{j,k_t} Y_{i,j} \cos(\theta_{i,j} + \delta_{j,k_t} - \delta_{i,k_t}), \forall k_t, i, j \quad (2)$$

$$\sum_{g\in G_i} Q_{g,k_t} W_{g,k_t} - PD_{i,k_t}^c K_1 V_{i,k_t}^{\beta_{k_t}^c} - [PD_{i,k_t}^r + PD_{i,k_t}^{rc}(P_{k_t}^{max}) - P_{k_t}^{LC}] K_2 V_{i,k_t}^{\beta_{k_t}^r} + \sum_{n\in N_i}(QC_{n,k_t}) = -\sum_j V_{i,k_t} V_{j,k_t} Y_{i,j} \sin(\theta_{i,j} + \delta_{j,k_t} - \delta_{i,k_t}), \forall k_t, i, j \quad (3)$$

The residential loads comprise fixed and controllable components; the fixed components (PD^r) are obtained from a forecasting engine, while the controllable components $PD^{rc}(P^{max})$ represent the dispatchable demand included in the MEMS model as a function of P^{max}, which is estimated using the RCLPE discussed in Section IV. Furthermore, residential and commercial loads are considered as a mix of constant impedance (Z), constant current (I) and constant power (P) (ZIP) loads, and are included in the MEMS model as exponential functions of the voltage, as shown in (2) and (3). Note that customers are not paid any incentives for DR participation by the MGO, but are assumed to be controlled

by an intelligent Home EMS (HEMS) designed to individually optimize their costs and/or energy consumption, as explained in detail in [18].

B. Reserve Constraint

This constraint ensures that the spinning reserve requirement for the microgrid is provided by the dispatched generators as follows:

$$\sum_g (\bar{P}_g - P_{g,k_t}) W_{g,k_t} \geq R^{sv} \sum_i [PD^c_{i,k_t} V^{\alpha^c_{k_t}}_{i,k_t} + [PD^r_{i,k_t} + PD^{rc}_{i,k_t}(P^{max}_{k_t}) - P^{LC}_{k_t}] V^{\alpha^r_{k_t}}_{i,k_t}], \forall k_t \quad (4)$$

C. Generalized UC Constraints

The following constraints include active and reactive power generation limits, ramp-up and ramp-down constraints, minimum up-time and down-time constraints, and coordination constraints:

$$\underline{P}_g W_{g,k_t} \leq P_{g,k_t} \leq \bar{P}_g W_{g,k_t}, \quad \forall g, k_t \quad (5)$$

$$\underline{Q}_g W_{g,k_t} \leq Q_{g,k_t} \leq \bar{Q}_g W_{g,k_t}, \quad \forall g, k_t \quad (6)$$

$$P_{g,k_t+\Delta t_{k_t}} - P_{g,k_t} \leq R^{up}_g \Delta t_{k_t} + U_{g,k_t+\Delta t_{k_t}} \underline{P}_g, \forall g, k_t \quad (7)$$

$$P_{g,k_t} - P_{g,k_t+\Delta t_{k_t}} \leq R^{dn}_g \Delta t_{k_t} + S_{g,k_t+\Delta t_{k_t}} \underline{P}_g, \forall g, k_t \quad (8)$$

$$(G^{on}_{g,k_t-\Delta t_{k_t}} - T^{up}_g)(W_{g,k_t-\Delta t_{k_t}} - W_{g,k_t}) \geq 0, \forall g, k_t \quad (9)$$

$$(G^{off}_{g,k_t-\Delta t_{k_t}} - T^{dn}_g)(W_{g,k_t} - W_{g,k_t-\Delta t_{k_t}}) \geq 0, \forall g, k_t \quad (10)$$

$$U_{g,k_t} - S_{g,k_t} = W_{g,k_t} - W_{g,k_t-\Delta t_{k_t}}, \quad \forall g, k_t \quad (11)$$

$$U_{g,k_t} + S_{g,k_t} \leq 1, \quad \forall g, k_t \quad (12)$$

D. Energy Storage System

The ESS constraints include the energy balance and constraints to prevent simultaneous charging/discharging, plus limits on SOC and charging/discharging power, as follows:

$$SOC_{n,k_t+\Delta t_{k_t}} - SOC_{n,k_t} = \left(P^{ch}_{n,k_t} \eta^{ch}_n - \frac{P^{dch}_{n,k_t}}{\eta^{dch}_n} \right) \Delta t_{k_t}, \quad \forall n, k_t \quad (13)$$

$$P^{ch}_{n,k_t} P^{dch}_{n,k_t} = 0, \quad \forall n, k_t \quad (14)$$

$$\underline{SOC}_n \leq SOC_{n,k_t} \leq \overline{SOC}_n, \quad \forall n, k_t \quad (15)$$

$$P^{ch}_{n,k_t} \leq \overline{PESS}_n, \quad \forall n, k_t \quad (16)$$

$$P^{dch}_{n,k_t} \leq \overline{PESS}_n, \quad \forall n, k_t \quad (17)$$

E. Grid Constraints

The following represent the grid operational constraints to ensure the bus voltages and apparent power transfers are within specified limits:

$$\underline{V} \leq V_{i,k_t} \leq \bar{V}, \quad \forall i, k_t \quad (18)$$

$$\mathcal{S}_{i,j,k_t}(|V_{i,k_t}|, |V_{j,k_t}|, |\delta_{i,k_t}|, |\delta_{j,k_t}|) \leq \overline{\mathcal{S}}_{i,j}, \quad \forall i, j, k_t \quad (19)$$

F. DR Cap

The following constraint imposes a limit on the maximum demand P^{max} at a given time interval:

$$\underline{P}^{max} \leq P^{max}_{k_t} \leq \bar{P}^{max}, \quad \forall k_t \quad (20)$$

where the minimum value $\underline{P}^{max}$ represents the minimum loading condition defined in agreement with DR participants, while the maximum value $\bar{P}^{max}$ specifies the maximum peak demand desired by the utility.

III. MEMS Implementation

Equations (1)-(20) represent the proposed MEMS model, and correspond to a Mixed Integer Non-linear Programming (MINLP) problem. This optimization problem is solved using the existing MINLP solvers, in particularly the DICOPT solver [19], and a warm start procedure, i.e., the previous feasible solution is used as the starting point of the next solution. If the problem is infeasible during the solution process, the binary decision variables W_{g,k_t} are re-initialized to the ON state and the optimization problem is re-solved.

It is important to note that DGs in microgrids generally have fast start-up, shut-down, and ramp characteristics in the order of a few minutes. In spite of that, constraints (7)-(10) need be considered because of the MPC recalculation time, which is less than the minimum up- or down-times, or the time required to ramp up to full capacity of the respective DGs. In the present work, the minimum up- and down-times of the diesel generators are assumed 30 minutes, and full capacity ramp-up and ramp-down rates of 10 minutes are used, which are typical values for diesel generators [20].

A. Decomposition Approach

The microgrid EMS problem can also be decomposed into UC and OPF sub-problems and solved sequentially, as proposed in [14]. The decoupled microgrid EMS (DMEMS) starts with the microgrid UC (MUC) sub-problem, which is solved considering the inputs provided by the forecasting engine and smart loads to obtain the commitment decisions. To accomplish this, the real power demand, supply balance, and reserve constraints are modified as follows:

$$\sum_g P_{g,k_t} W_{g,k_t} + \sum_i (PV_{i,k_t} + PW_{i,k_t}) + \sum_n (P^{dch}_{n,k_t} - P^{ch}_{n,k_t}) = \sum_i [PD^c_{i,k_t} + PD^r_{i,k_t} + PD^{rc}_{i,k_t}(P^{max}_{k_t}) - P^{LC}_{k_t}], \forall k_t \quad (21)$$

$$\sum_g (\bar{P}_g - P_{g,k_t}) W_{g,k_t} \geq R^{sv} \sum_i [PD^c_{i,k_t} + PD^r_{i,k_t} + PD^{rc}_{i,k_t}(P^{max}_{k_t}) - P^{LC}_{k_t}], \forall k_t \quad (22)$$

Hence, the MUC sub-problem is comprised of (1), (5)-(17), (20), (21) and (22). The optimal decisions thus obtained are then applied to the microgrid OPF (MOPF) sub-problem, comprised of (1)-(8), (13)-(20), to obtain the optimal dispatch

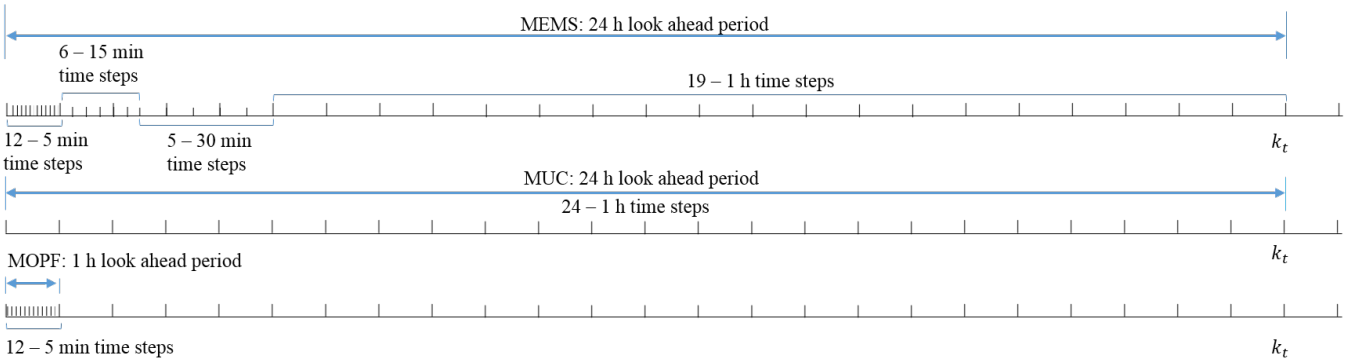

Fig. 2. Time horizons of MEMS, MUC and MOPF models.

decisions that are implemented as reference set points for controllable DERs.

B. Time Horizons

Solving the MEMS problem considering a uniform time horizon of 5 min intervals over 24 hours, i.e., T = 288 intervals, adds to the computational burden. In this work, therefore, a non-uniform time scale comprising a higher resolution for the first few min and reduced resolution in the later part is considered for the MEMS model, as in [14]. This accounts for the fact that the accuracy of forecasts vary over the forecasting horizon; thus, the shorter the horizon, the more accurate the forecast than that over an extended horizon. The considered non-uniform time horizon is shown in Fig. 2, yielding 12 time steps of 5 min, followed by 6 time steps of 15 min, and 5 time steps of 30 min, and finally 19 time steps of 1 hour, all adding to a total of 24 hours.

For the DMEMS framework, the MUC problem is solved for a 24 hour look ahead time window with a uniform time resolution of one hour, as shown in Fig. 2, as decisions related to UC problem follow slower dynamics. The MOPF problem is, on the other hand, solved with a look ahead period of one hour and uniform time resolutions of 5 min.

C. MPC Implementation

The optimal decisions obtained by solving the MEMS model over the horizon $\tau_0 = \{0, \ldots, T\}$ relies on the forecasted inputs of intermittent energy sources and demand. In isolated microgrids, renewable power generation forecasts can vary significantly over a 24 hour time horizon. Hence, the optimal decision of the MEMS must be re-calculated with updated forecasted inputs every 5 min, based on an MPC approach. In this case, the optimal results obtained by solving the MEMS model are applied only to the next time interval, after which the forecast inputs are updated and the MEMS model is re-solved over the next 24 hour horizon, repeating this process every 5 min [13], [14].

IV. Residential Controllable Load Profile Estimator

In this work, the smart residential DR options discribed in [18] is considered, in which a household owns an intelligent

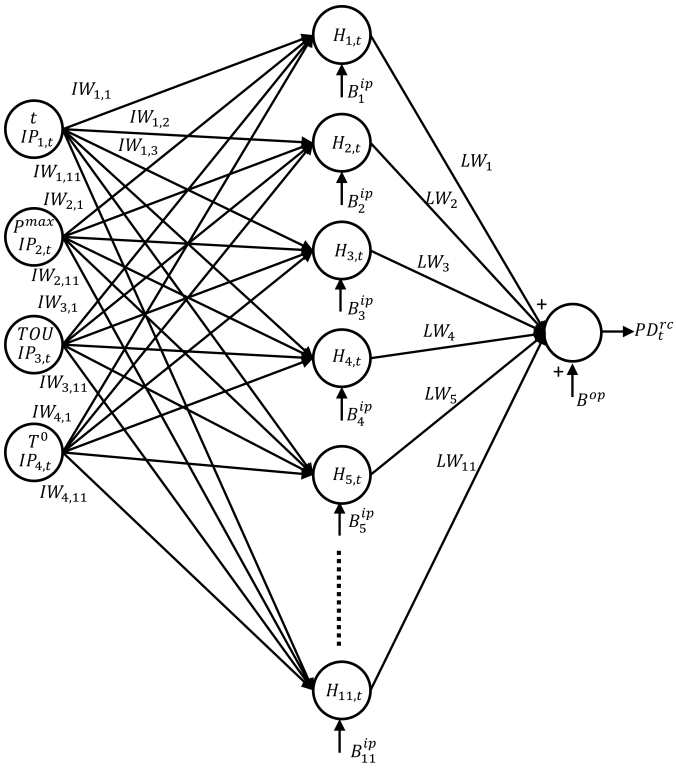

Fig. 3. Smart load NN model obtained from the RCLPE.

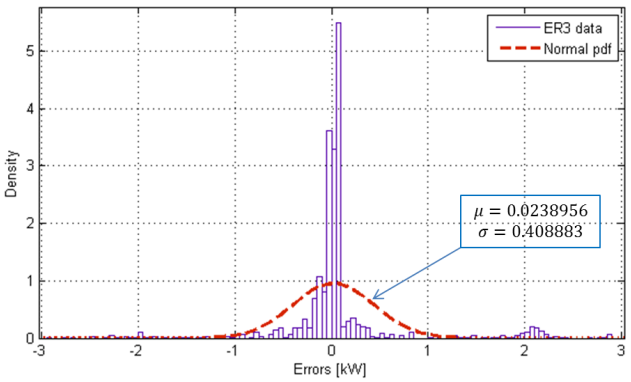

Fig. 4. Validation error histogram for RCLPE model.

HEMS or EHMS for optimally managing the household loads to reduce electricity costs and/or consumption. It is assumed here that such EHMS is connected to the microgrid with a bi-directional communication network, so that the MGO can send DR control signals, in particular P^{max}, to the EHMS. Thus, the EHMS would schedule the operation of the household based on the DR signal, weather conditions, and customer preferences. This EHMS is comprised of an objective function seeking to minimize the customer's energy cost and/or consumption, subject to operational constraints of the household appliances and constraints associated with DR controls. The DR control signal P^{max} is determined by the MGO using the proposed MEMS model to limit the PD^{rc} of each house with an EHMS, within certain limits.

For efficient energy management of a microgrid in the presence of DR, the PD^{rc} profile needs to be properly estimated, so that an adequate DR model can be integrated in the MEMS framework. Thus, based on the universal approximation theorem [21], which states that a single hidden layer NN can be used to approximate any arbitrary continuous function, an RCLPE is developed to estimate the PD^{rc} from ambient temperature, TOU price, time of day and P^{max} inputs.

A supervised learning technique is applied to train the NN with measured data from smart meters and simulated data for an actual EHMS. These data were obtained for the months of May, June, and July of 2012 for weekdays, with a resolution of 5 min, and includes actual temperature profiles, TOU prices, and load profiles for different P^{max} values. An input 121,537 x 4 matrix and a 121,537 output vector is used for training the NN. Ultimately, the estimated PD^{rc} NN can be expressed as a function of time, ambient temperature, TOU price, and P^{max}, as follows:

$$PD_t^{rc} = f(t, P^{max}, TOU, T^0) \tag{23}$$

By varying the number of hidden layer neurons and training the NN with the available data, the best result is obtained with 11 hidden layer neurons, using the Levenberg-Marquardt learning technique in MATLAB^{TM}, because of its robust nature [22]. The resulting RCLPE structure, shown in Fig. 3, has an R^2 of 0.87 for the complete dataset, indicating that the output of the NN and the data used for training have a high correlation. Note that the complexity of the NN-model obtained, reflects the complex relations between the various inputs to the load model and the power demand. Hence, the simpler models (e.g., linear) would not have been able to properly represent the controllable load modeled here.

After the training procedure, the NN model is validated and tested with the datasets that are not used for training, to evaluate the performance of the NN. Figure 4 shows the validation error histogram for the proposed NN model in Fig. 3, depicting the maximum and minimum possible error and their number of occurrences; observe that the model is quite accurate, with about 80% errors being within the range of $\pm$ 0.2 kW for a peak power of about 5 kW.

The mathematical model needed in the proposed MEMS model to represent the smart load demand PD^{rc}, which is the output from the NN model, can be expressed as an equation

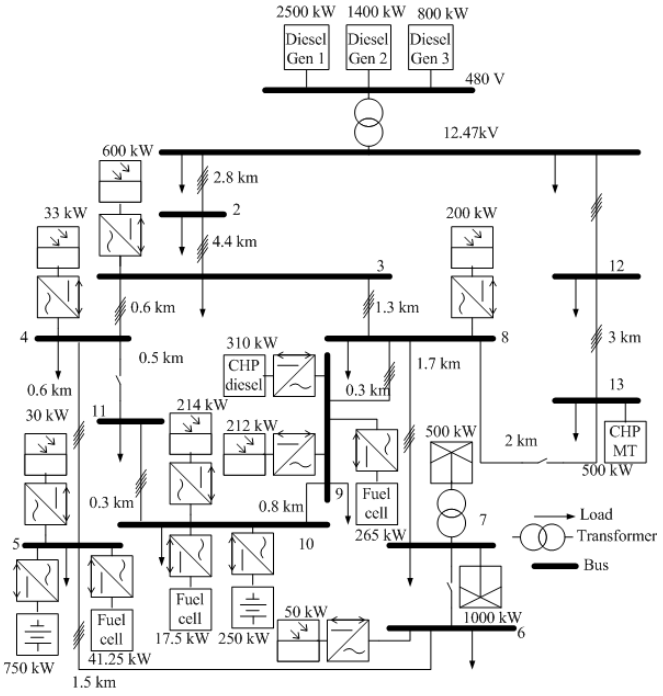

Fig. 5. Modified CIGRE microgrid benchmark [14].

as follows:

$$PD_t^{rc} = \sum_{y \in Y} \left(\frac{2}{1 + e^{-2H_{y,t}}} - 1 \right) LW_y + B^{op}, \forall t \tag{24}$$

where

$$H_{y,t} = \sum_{x \in X} IP_{x,t} IW_{x,y} + B_y^{ip}, \forall y \in Y \tag{25}$$

It should be mentioned that other types of controllable/smart loads, beside the EHMS, could be modeled in a similar way, with an appropriately NN model. Therefore, the proposed approach can be considered generic in this regard, with the only requirement for the smart load being that it should be able to respond to peak demand commands, as, for example, the case of Peak Saver Plus loads [23].

V. Results And Discussion

To validate the proposed MEMS for a significantly complex isolated microgrid, the modified CIGRE medium voltage benchmark network shown in Fig. 5 is considered, based on the test microgrid used in [14] with 25% more total ESS capacity, and including the main transformer limit. To represent an isolated microgrid, the connection to the main grid at Bus 1 is replaced with 3 diesel units of a combined capacity of 4,700 kW. The total installed capacity in the microgrid is 9,216 kW including ESS, intermittent energy sources and various other DGs. In order to account for the uncertainties and errors in the forecast of the renewables and demand, probability density functions (pdf) for day and 1-hour ahead are used to obtain the wind, PV, and demand power profiles, based on linear approximations of the difference between the 24-hour and 1-hour ahead forecast errors with respect to time.

TABLE I
SUMMARY OF RESULTS WITH MEMS

DR control [%]	Objective function [$]	Energy served by ESS [kWh]	Energy curtailed [kWh]	Load factor	Peak demand [kW]
0	83,781	3,037	528	0.580	7,575
20	62,447	2,870	351	0.589	7,431
40	42,464	2,808	185	0.6	7,287
60	25,099	2,760	41	0.611	7,141
100	19,941	2,416	0	0.631	6,851

TABLE II
SUMMARY OF RESULTS WITH DMEMS

DR control [%]	Objective function [$]	Energy served by ESS [kWh]	Energy curtailed [kWh]	Load factor	Peak demand [kW]
0	315,354	1,097	2,468	0.568	7,576
20	289,379	1,067	2,252	0.578	7,431
40	263,168	1,064	2,034	0.589	7,286
60	241,396	1,033	1,853	0.6	7,141
100	195,833	1,053	1,474	0.622	6,851

In the RCLPE, the EHMS is considered to be managing four household appliances, namely, dish washer, cloth dryer, washer, and air conditioner. It is assumed that 50% of the total energy demand of households, which corresponds to 30% of the total energy demand of the microgrid, is from controllable loads.

A. Case Studies

The proposed MPC based MEMS framework is validated for 24 hours of operation, with a re-calculation time of 5 min. The MEMS model and the MUC and MOPF models, as part of the DMEMS framework, were coded in GAMS [24]. The MEMS and MUC models, being mixed integer non-linear programming (MINLP) problems (due to the smart load NN model in the MUC), are solved using the DICOPT solver [19], which first solves the relaxed MINLP problem where the binary variables are relaxed and considered as continuous variables. To obtain the best integer solution, the DICOPT solves MIP and NLP sub-problems sequentially, multiple times, until the NLP solution starts deteriorating [19]. Although the DICOPT solver obtains the global optimal solutions for both convex and non-convex models [19], there is no guarantee that the global optimal solution will be reached. Nevertheless, sub-optimal solutions obtained for the EMS models, are all that is needed in practice for microgrid operation. The MOPF is a non-linear programming (NLP) problem that is solved using the SNOPT solver [19].

To investigate the impacts of DR on microgrid operation, different cases, from no controllable loads to 100% EHMS loads (30% of total demand), are considered, where EHMS loads in the microgrid are controlled by an optimal P^{max}. Note that, 20% controllable loads means that 6% of the total energy demand of the microgrid is being controlled through an optimal P^{max}.

The proposed MEMS model using the MPC approach required on average 28 s to solve for a single 24 hour variable time-steps horizon, in a Intel(R) Xeon(R) CPU L7555 1.87GHz (4 processors) server, which is well within the 5 min MPC re-calculation time. This was repeated 288 times by shifting the time horizon forward by 5 min, for 24 hours, thus simulating the MEMS operation in 1 full day; this computation took 180 min. On the other hand, the DMEMS framework required a total computation time of around 30 min, with an average of 6.25 s per iteration. Although, the MEMS framework requires a longer simulation time than the DMEMS framework, it is still reasonable for real-time applications.

Table I presents a summary of the results obtained from the MEMS application, which shows that as DR control increases, the energy curtailed by the MGO decreases, with no need for load curtailment for 100% DR control. Consequently, the total operating costs are very high without DR control, because of the high cost of load curtailment, decreasing as DR is increased. Furthermore, the load factor, which represents the ratio of average daily demand with respect to peak demand, increases from 0.580 to 0.631, indicating that the load profile gets flatter as DR control increases. Finally, and as expected, the peak demand decreases from 7.5 MW to 6.8 MW with increased DR control.

From the summary of results presented for the DMEMS framework in Table II, it can be observed that with increased DR control, peak demand decreases from 7.5 MW to 6.8 MW, and the load factor increases from 0.568 to 0.622, which are similar to the results to those presented in Table I for the proposed MEMS approach. However, note that even though the total cost in DMEMS decreases with increased DR control, it is considerably higher than the total cost obtained with the MEMS approach, due to comparatively high load curtailment. Furthermore, observe that the total energy served by ESS with the MEMS approach is higher than with the DMEMS, which indicates the MEMS method makes effective use of the ESS in the dispatch, hence requiring less load curtailment.

The optimal dispatch of the DERs determined from the two EMS MPC approaches for a 24 h interval, considering P^{max} feedback or not, are presented in Figs. 6 and 7. The negative area shows the total charging energy absorbed by the ESS, and white spaces under the demand (PD) line show the curtailed energy, confirming the better use of ESS and less load curtailment with the proposed MEMS approach. Particularly, two important time windows are highlighted in Figs. 6 and 7:

- In Window 2, between hours 22 to 22.5, a peak demand of 7.4 MW is observed when there is no P^{max} control, because the EHMS shifts its controllable demand to these hours when the TOU price is low. On the other hand, with P^{max} control, the EHMS manages the load demand such that the peak is reduced to 5.8 MW, hence reducing load curtailment significantly.
- Note in Window 1 of Fig. 6 that the ESSs are charged to store energy until hour 6, and are dispatched to meet the high demand between hours 6 and 7. On the other hand, for the DMEMS approach, as shown in Fig. 7, the demand is not fully met by the DGs and ESSs from hour 6 to 7, thus requiring load curtailment, which is due to the

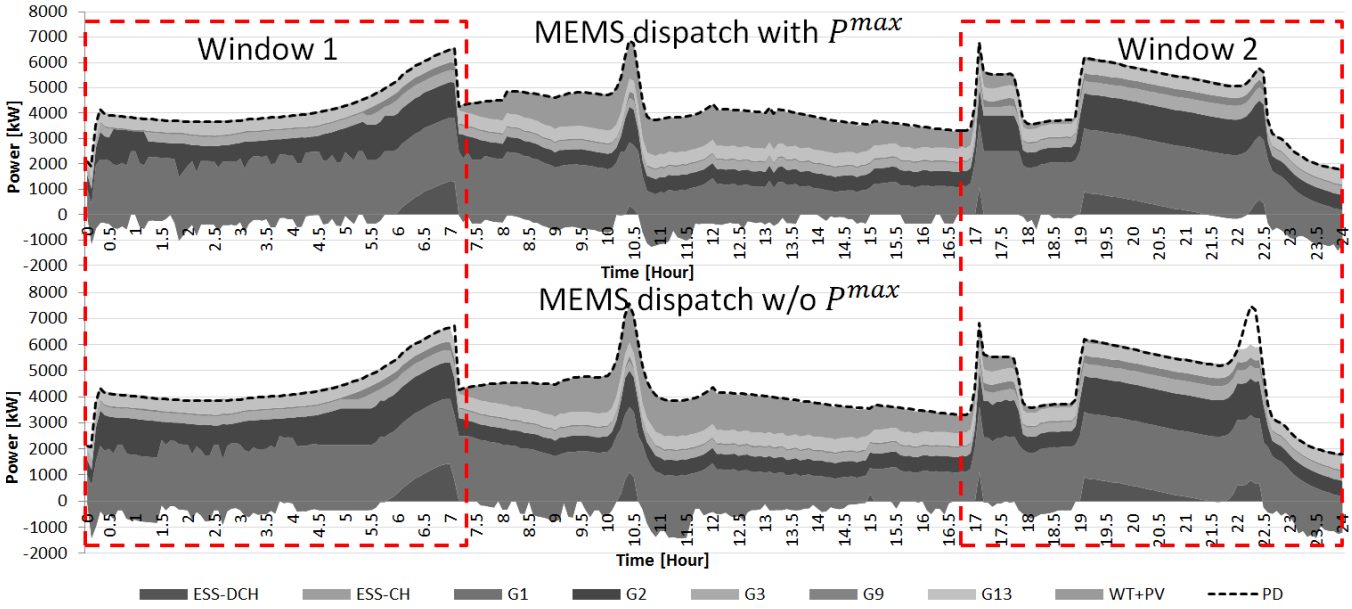

Fig. 6. Optimal dispatch obtained from the MEMS approach with and without P^{max}.

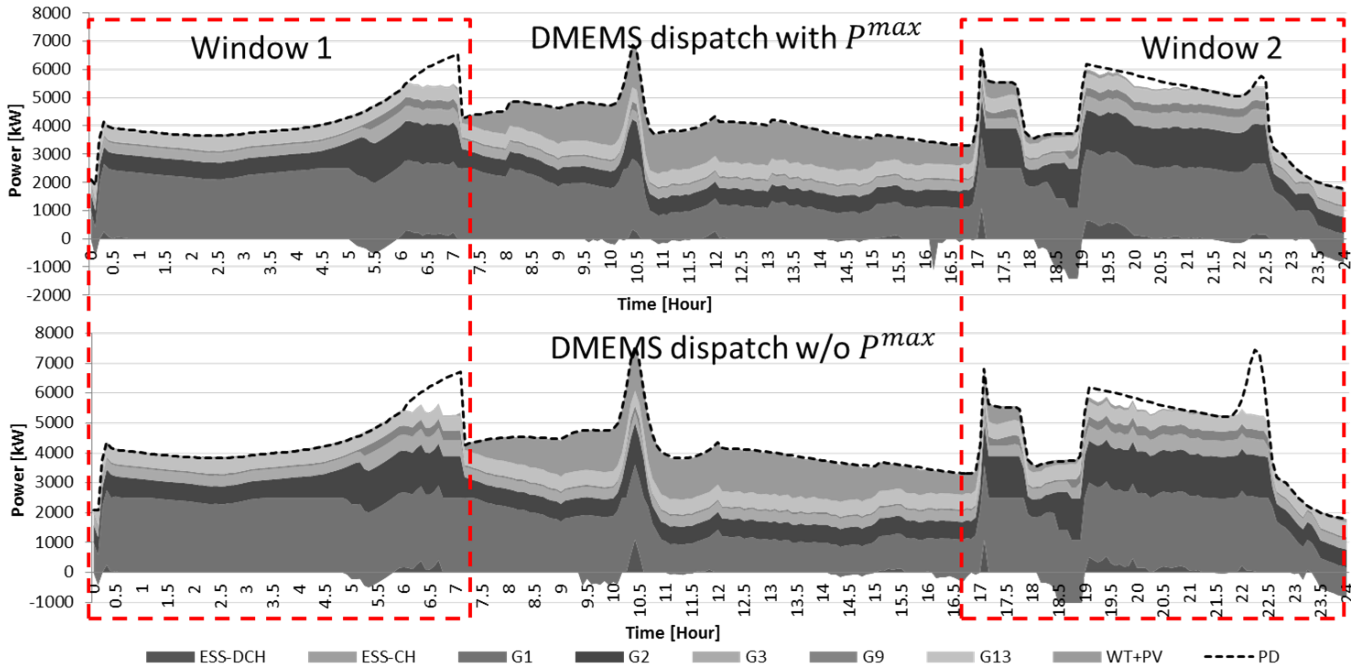

Fig. 7. Optimal dispatch obtained from the DMEMS approach with and without P^{max}.

ESSs not being optimally scheduled for charging during off-peak hours.

- When energy is available from renewables between hours 7 and 17, the MEMS approach schedules more ESSs charging (Fig. 6), which are dispatched to meet the demand in Window 2. However, in the DMEMS approach (Fig. 7), the ESSs are not adequately charged to serve the peak demand, and hence load curtailment is required from hour 19 to 22.5 due to lack of generation from DGs. Even though load curtailment is still needed without P^{max} control in the MEMS approach, it is lower compared to that with the DMEMS framework.

In Fig. 8 the 24 h optimal P^{max} profile obtained from the MEMS approach and the TOU price profiles are depicted.

B. *Effect of Uncertainties in the RCLPE Model*

As discussed in Section IV, there are errors associated with the NN-based smart load model. Therefore, to study the effect of these errors in the proposed dispatch approach, a real-time operation scenario is considered here. The errors γ_{k_t} in the output of the NN-based model are considered in the MEMS, based on a normalized pdf of the validation error histogram

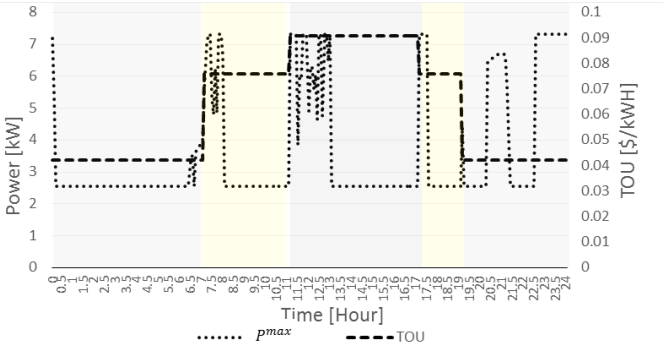

Fig. 8. Optimal P^{max} obtained from MEMS approach and TOU prices.

TABLE III
SUMMARY OF RESULTS FOR DETERMINISTIC AND STOCHASTIC LOAD MODEL

Load Model	Objective function [$]	Energy served by ESS [kWh]	Total demand [kWh]	Load factor	Peak demand [kW]
Deterministic	19,941	2,416	103,822	0.631	6,851
Stochastic	20,098	2,480	104,626	0.641	6,799

as shown in Fig. 4. Note that this approximate pdf overstates the actual error distribution in the model, thus representing a worst case scenario for testing purposes. These errors are applied as a stochastic deviation parameter of the controllable demand as follows:

$$PD^{rc}_{i,k_t} = \widehat{PD}^{rc}_{i,k_t}(P^{max}_{k_t}) + \gamma_{k_t} \tag{26}$$

where $\widehat{PD}^{rc}_{i,k_t}$ represents the deterministic output of the NN model (24).

The MEMS model including (26) is validated considering 100% EHMS loads with P^{max} control for 24 hour of operation using the MPC approach, and the obtained results are summarized in Table III, and compared with the deterministic load model, which does not consider uncertainties in the output of the RCLPE. Observe that there is less than 1% changes in the operating cost and peak demand; moreover, the change in the load factor is only 1.5%. Furthermore, from the dispatch solution shown in Fig. 9, note that there are no significant changes in the dispatch compared to the schedule obtained for the base case with P^{max} control shown in Fig. 6, showing that errors in the output of the RCLPE have little impact on the dispatch solutions obtained with the proposed MEMS.

VI. CONCLUSIONS

In this paper, an NN-based model has been proposed to estimate controllable loads demand as a function of ambient temperature, TOU prices, time of the day, and demand limit. This developed mathematical model was integrated in a proposed comprehensive MEMS framework, which was formulated considering UC operational and network flow constraints simultaneously. The deviations in the forecast of the renewables and electricity demand were managed by adopting an MPC approach. To evaluate the benefits of the proposed MEMS approach, an DMEMS approach was implemented by decomposing the EMS problem into UC and OPF subproblems.

The MEMS and DMEMS techniques were compared on a CIGRE benchmark system, demonstrating that, even though the MEMS method took longer to solve than that of the DMEMS approach, better overall dispatch results were obtained, with less load curtailment and better use of ESS resources, within feasible computational times for real-time applications. Furthermore, the solutions obtained with both the EMS methodologies for a smart load highlighted the advantages of DR schemes, in particular with respect to reduction in peak demand, load curtailment, total costs, and improvements in load factors, demonstrating that the proposed DR scheme enhances the microgrid's load serving capability in the long run without the need for large investments. Finally, it is shown that undesirable load spikes at low electricity price hours due to customer response can be mitigated with the proposed approach.

ACKNOWLEDGMENT

The authors would like to thank Dr. Isha Sharma currently at Oak Ridge National Laboratory, Oak Ridge, TN, USA, for her help in the development of the NN-based smart load model.

REFERENCES

[1] R. Lasseter, "Microgrid," in *Proc. IEEE Power Engineering Soc. Winter Meet.*, vol. 1, Jan. 2002, pp. 305–308.
[2] F. Katiraei, R. Iravani, N. Hatziargyriou, and A. Dimeas, "Microgrids management: Controls and operation aspects of microgrids," *IEEE Power Energy Mag.*, vol. 6, no. 3, pp. 54–65, May/Jun 2008.
[3] IEEE-PES Task Force on Microgrid Control, "Trends in microgrid control," *IEEE Trans. Smart Grid*, vol. 5, no. 4, pp. 1905–1919, Jul. 2014.
[4] C. Chen, S. Duan, T. Cai, B. Liu, and G. Hu, "Smart energy management system for optimal microgrid economic operation," *IET Renewable Power Generation*, vol. 5, no. 3, pp. 258–267, 2011.
[5] H. Kanchev, F. Colas, C. Lazarov, and B. Francois, "Emission reduction and economical optimization of an urban microgrid operation including dispatched PV-based active generators," *IEEE Trans. Sustainable Energy*, vol. 5, no. 4, pp. 1397–1405, Oct. 2014.
[6] S. Y. Derakhshandeh, A. S. Masoum, S. Deilami, M. A. S. Masoum, and M. E. H. Golshan, "Coordination of generation scheduling with PEVs charging in industrial microgrids," *IEEE Trans. Power Syst.*, vol. 28, no. 1, pp. 102–111, Feb. 2013.
[7] S. Conti, R. Nicolosi, S. A. Rizzo, and H. H. Zeineldin, "Optimal dispatching of distributed generators and storage systems for MV islanded microgrids," *IEEE Trans. Power Delivery*, vol. 27, no. 3, pp. 1243–1251, May 2012.
[8] "Assesment of demand response and advanced metering," FERC Staff Report, Tech. Rep., Dec. 2012. [Online]. Available: http://www.ferc.gov/legal/staff-reports/12-20-12-demand-response.pdf
[9] A. Safdarian, M. Fotuhi-Firuzabad, and M. Lehtonen, "Benefits of demand response on operation of distribution networks: A case study," *IEEE Syst. Journal*, vol. 27, no. 3, pp. 1243–1251, May 2012, to appear.
[10] I. Sharma, K. Bhattacharya, and C. Cañizares, "Smart distribution system operations with price-responsive and controllable loads," *IEEE Trans. Smart Grid*, vol. 6, no. 6, pp. 795–807, Mar. 2015.
[11] A. Safdarian, M. Fotuhi-Firuzabad, and M. Lehtonen, "Integration of price-based demand response in DisCos' short-term decision model," *IEEE Trans. Smart Grid*, vol. 5, no. 5, pp. 2235–2245, Sep. 2014.
[12] K. Dietrich, J. M. Latorre, L. Olmos, and A. Ramos, "Demand response in an isolated system with high wind integration," *IEEE Trans. Smart Grid*, vol. 27, no. 1, pp. 20–29, Feb. 2012.
[13] R. Findeisen, "Nonlinear model predictive control: A sampled-data feedback persepective," Ph.D. dissertation, Univ. Stuttgart, Stuttgart, Germany, 2004.

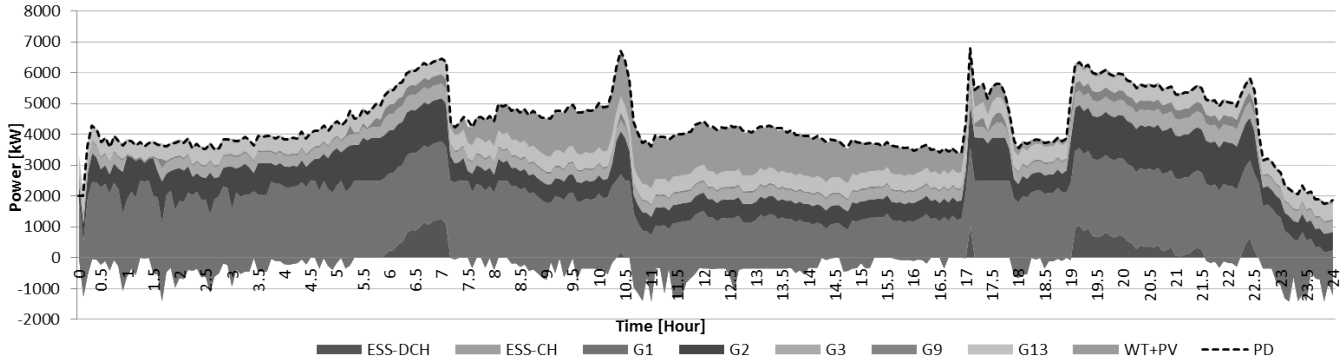

Fig. 9. Optimal dispatch obtained from the MEMS approach including errors in the estimation of PD^{rc}.

[14] D. E. Olivares, C. A. Cañizares, and M. Kazerani, "A centralized energy management system for isolated microgrids," *IEEE Trans. Smart Grid*, vol. 5, no. 4, pp. 1864–1875, Jul. 2014.

[15] R. Palma-Behnke, C. Benavides, F. Lanas, B. Severino, L. Reyes, J. Llanos, and D. Saez, "A microgrid energy management system based on the rolling horizon strategy," *IEEE Trans. Smart Grid*, vol. 4, no. 2, pp. 996–1006, Jun. 2013.

[16] A. Parisio, E. Rikos, and L. Glielmo, "A model predictive control approach to microgrid operation optimization," *IEEE Trans. Control Syst. Technol.*, vol. 22, no. 5, pp. 1813–1827, Sep. 2014.

[17] Energy hub management system. [Online]. Available: http://www.energyhub.uwaterloo.ca

[18] M. C. Bozchalui, S. A. Hashmi, H. Hassen, C. A. Cañizares, and K. Bhattacharya, "Optimal operation of residential energy hubs in smart grids," *IEEE Trans. Smart Grid*, vol. 3, no. 4, pp. 1755–1766, Dec. 2012.

[19] "GAMS–The solver manuals," Tech. Rep., Oct. 2015. [Online]. Available: http://www.gams.com/help/topic/gams.doc/solvers/allsolvers.pdf

[20] R. J. Yinger, "Behavior of Capstone and Honeywell microturbine generators during load changes, Ernest Orlando Lawrence Berkeley National Lab." Tech. Rep., Feb. 2004. [Online]. Available: http://www.certs.lbl.gov/pdf/49095.pdf

[21] F. Scarselli and A. C. Tsoi, "Universal approximation using feedforward neural networks: A survey of some existing methods, and some new results," *Journal on Neural Networks*, vol. 11, no. 1, pp. 15–37, Jan. 1998.

[22] M. Beale, M. T. Hogan, and H. B. Demuth, "Neural network toolbox," Neural Network Toolbox, The Math Works, pp. 5–25, 1992.

[23] Peaksaver plus. [Online]. Available: https://www.peaksaver.com/

[24] R. E. Rosenthal, "GAMS–A user's guide," Tech. Rep., May 2015. [Online]. Available: http://www.gams.com/dd/docs/bigdocs/GAMSUsersGuide.pdf

Bharatkumar V Solanki (S'14) received the Bachelor's degree in electrical engineering from Gujarat University, Ahmedabad, India in 2009 and Master's degree in Electrical Engineering from the Maharaja Sayajirao University of Baroda, Vadodara, India in 2011.

He worked as an analog hardware design engineer in ABB Global Industries and Service Limited, India from 2011 to 2013. He is currently working toward the Ph.D. degree in Electrical and Computer Engineering at the University of Waterloo, Waterloo, ON, Canada. His research interests include modeling, simulation, control and optimization of power systems.

Akash Raghurajan obtained his B.Tech degree from SASTRA University, India, and Master of Applied Science (MASc) degree from University of Waterloo, in 2012, and 2014, respectively.

Currently, he is working as an Edison engineer - software in General Electric, Canada. His current research interests include demand response, microgrids and Artificial Intelligent modeling.

Kankar Bhattacharya (M'95-SM'01) received the Ph.D. degree in electrical engineering from the Indian Institute of Technology, New Delhi, India, in 1993.

He was with the Faculty of Indira Gandhi Institute of Development Research, Mumbai, India, from 1993 to 1998, and with the Department of Electric Power Engineering, Chalmers University of Technology, Gothenburg, Sweden, from 1998 to 2002. In 2003, he joined the Electrical and Computer Engineering Department, University of Waterloo, Waterloo, ON, Canada, where he is currently a Full Professor. His current research interests include power system economics and operational aspects.

Claudio A. Cañizares (S'85-M'91-SM'00-F'07) received the Diploma degree in electrical engineering from Escuela Politcnica Nacional, Quito, Ecuador, and the M.S. and Ph.D. degrees in electrical engineering from the University of WisconsinMadison, Madison, WI, USA, in 1984, 1988, and 1991, respectively.

He has held various academic and administrative positions with the Electrical and Computer Engineering Department, University of Waterloo, Waterloo, ON, Canada, since 1993, where he is currently a Full Professor, the Hydro One Endowed Chair, and the Associate Director of the Waterloo Institute for Sustainable Energy. His current research interests include modeling, simulation, control, stability, computational, and dispatch issues in sustainable power and energy systems in the context of competitive markets and smart grids.

Dr. Cañizares was the recipient of the Hydro One Research Chair Award in 2010 and several IEEE Power and Energy Society (PES) Working Group Awards, and has held several leadership appointments in the IEEE PES Technical Committees and Subcommittees. He has been a Fellow of the Royal Society of Canada since 2012 and a Registered Professional Engineer in the province of Ontario since 1995.